Manufacturing Letters 38 (2023) 60–64

Contents lists available at ScienceDirect

Manufacturing Letters

journal homepage: www.elsevier.com/locate/mfglet

Letters

On the use of machine learning and genetic algorithm to predict the region processed by laser peen forming

Siva Teja Sala [a,*], Richard Körner [b], Norbert Huber [a,b], Nikolai Kashaev [a]

[a] Institute of Materials Mechanics, Helmholtz-Zentrum Hereon, Max-Planck Str. 1, 21502 Geesthacht, Germany
[b] Institute of Materials Physics and Technology, Hamburg University of Technology, Eißendorfer Straße 42, 21073 Hamburg, Germany

ARTICLE INFO

Article history:
Received 13 July 2023
Received in revised form 17 September 2023
Accepted 18 September 2023
Available online 22 September 2023

Keywords:
Laser peen forming
Machine learning
Cellular automata neural network
Genetic algorithm

ABSTRACT

Laser peen forming uses laser-pulse-induced strains to deform sheets by adjusting laser parameters and peening patterns. Finding an optimal pattern in a vast space of practically infinite solutions is challenging. This study presents a workflow using a simplified model to predict deformation. A machine learning-based cellular automata neural network (CANN) and genetic algorithm (GA) were used for pattern prediction. Experiments showed high process uncertainty, justifying simplified modeling. The CANN predicted patterns reliably but lacked generalization due to insufficient deformation data for various process parameters. The GA required optimization efforts to reduce computation time but was successful at generalizing pattern prediction.

© 2023 The Authors. Published by Elsevier Ltd on behalf of Society of Manufacturing Engineers (SME). This is an open access article under the CC BY license (http://creativecommons.org/licenses/by/4.0/).

1. Introduction

Laser peen forming (LPF) is a sheet metal forming technique that utilizes laser-induced shock waves applied to a surface region to obtain a global deformation in the specimen [10,7]. The application of shock waves induces plastic strain in the upper surface of the treated area, leading to deformation in the surrounding material as it adjusts to accommodate the mismatched plastic strain. LPF is widely known to be applicable to a wide range of thin-sheet metals such as aluminum alloys [2], titanium alloys [15,10], and metal fiber laminates [11]. Depending on the material properties, sheet thickness, and process parameters, LPF can bend thin sheets in different directions i.e. convex or concave relative to the direction of the laser beam [10]. The treated region, or peening pattern, is also a crucial LPF parameter that significantly affects deformation. Choosing the best peening pattern presents a considerable challenge for the application of LPF (referred to as the '*inverse problem*'). Typically, the peening pattern is selected through a process of experimentation, trial, and error, and human intuition. This approach inherently increases the effort required to identify the appropriate peening pattern and to achieve the desired shape. Without a systematic method for pattern selection, the process becomes impractical due to time and resource limitations. Therefore, there is a need for efficient approaches to find the optimal treatment region during LPF.

To overcome the extensive experimental effort required, the impact of the peening pattern can be predicted using FE simulations, employing the well-established '*Eigenstrain*' approach [6]. This approach allows for the modeling of the combined effects of multiple laser pulses on large specimens, offering computational efficiency and accuracy in capturing the global deformation. Yet, this methodology still necessitates FE simulation of residual stresses or plastic strains generated in smaller peening which by themselves remains computationally demanding [14]. Nevertheless, simplification of the eigenstrain approach has been found by approximating the in-plane eigenstrain profiles in the case of shot peen forming, which is similar to the LPF process [4,16]. The present study utilizes a simplified FE simulation strategy that employs a linear-elastic predictive model to predict the deformation occurring in the treated region with sufficient accuracy. The simplified approach is computationally efficient and does not require strain measurements for verification, increasing its accessibility. Instead of computationally expensive simulations of smaller peening patches and extracting the plastic strains [14], this simplified approach iteratively adjusts stress values in the treated regions until deformed results from the simulation match the experimentally obtained deformation. The reduced computation time of the simplified FE simulation makes this iterative adjustment feasible.

Studies have already explored the use of optimization methods [8,9] for LPF and multi-layer perceptron model [16] for shot peen

* Corresponding author.
E-mail address: siva.sala@hereon.de (S.T. Sala).

https://doi.org/10.1016/j.mfglet.2023.09.006
2213-8463/© 2023 The Authors. Published by Elsevier Ltd on behalf of Society of Manufacturing Engineers (SME).
This is an open access article under the CC BY license (http://creativecommons.org/licenses/by/4.0/).

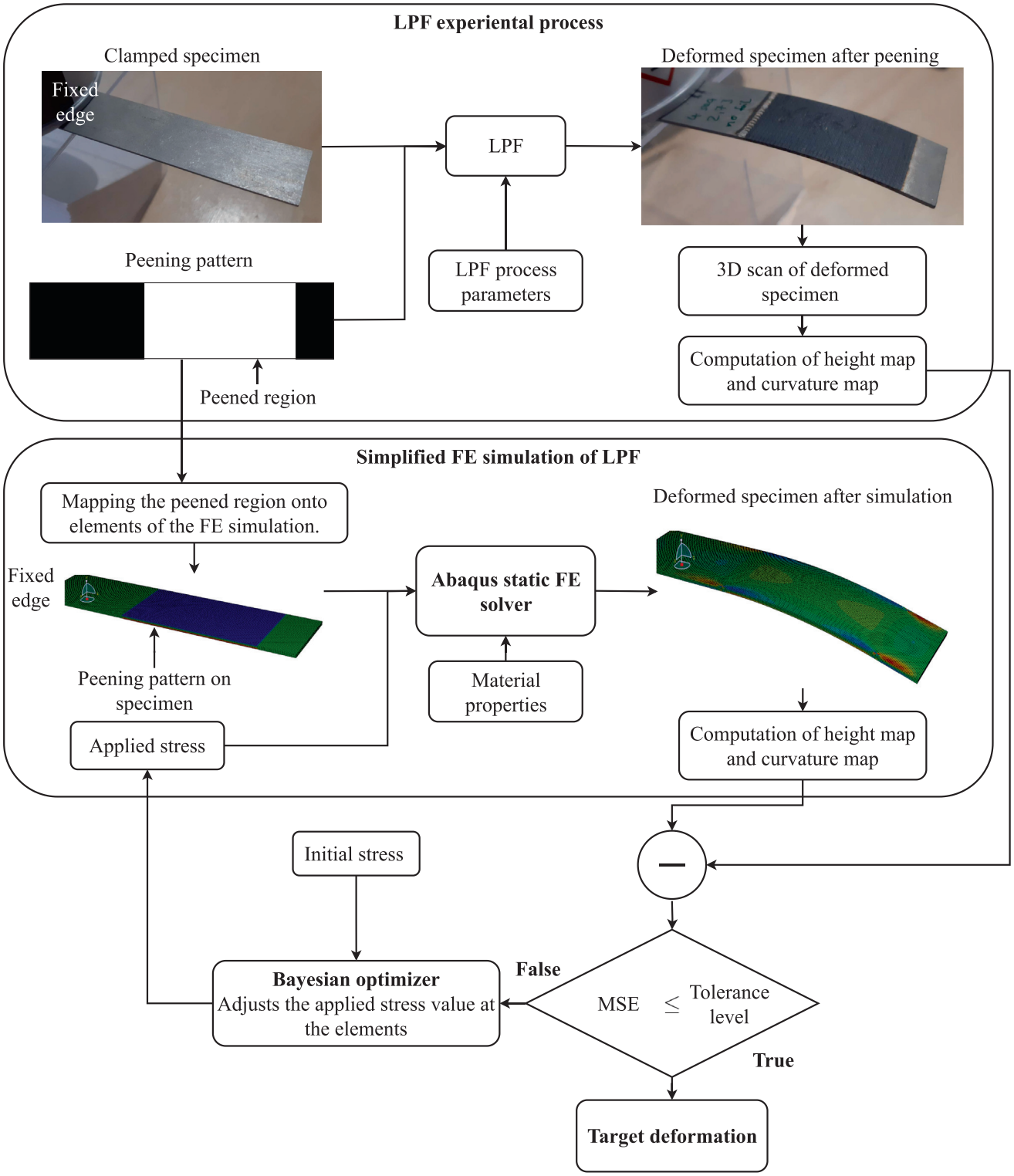

Fig. 1. This flowchart outlines the FE simulation workflow for LPF. A peening experiment with desired parameters yields a deformed specimen, which is 3D-scanned using Creaform HandySCAN 3D. Height and curvature maps are sampled from the scan results. The peening pattern image is mapped onto corresponding elements in the FE simulation. An initial stress value is applied to the treated region, and height and curvature maps are computed. The MSE, representing the difference between the FE simulation and experiment, is calculated. The Bayesian optimizer adjusts the applied stress value to minimize the MSE, iteratively improving until the desired tolerance level is reached.

forming to identify peening patterns under specific process conditions, aiming to achieve complex shapes. Nevertheless, these methods need substantial implementation and computation efforts [8] and have the requirement of a large dataset [16]. This work introduces a simulation workflow that enables faster generation of experimentally validated simulations and the development of models with fewer data, addressing the limitations of existing literature. The present study proposes two approaches:

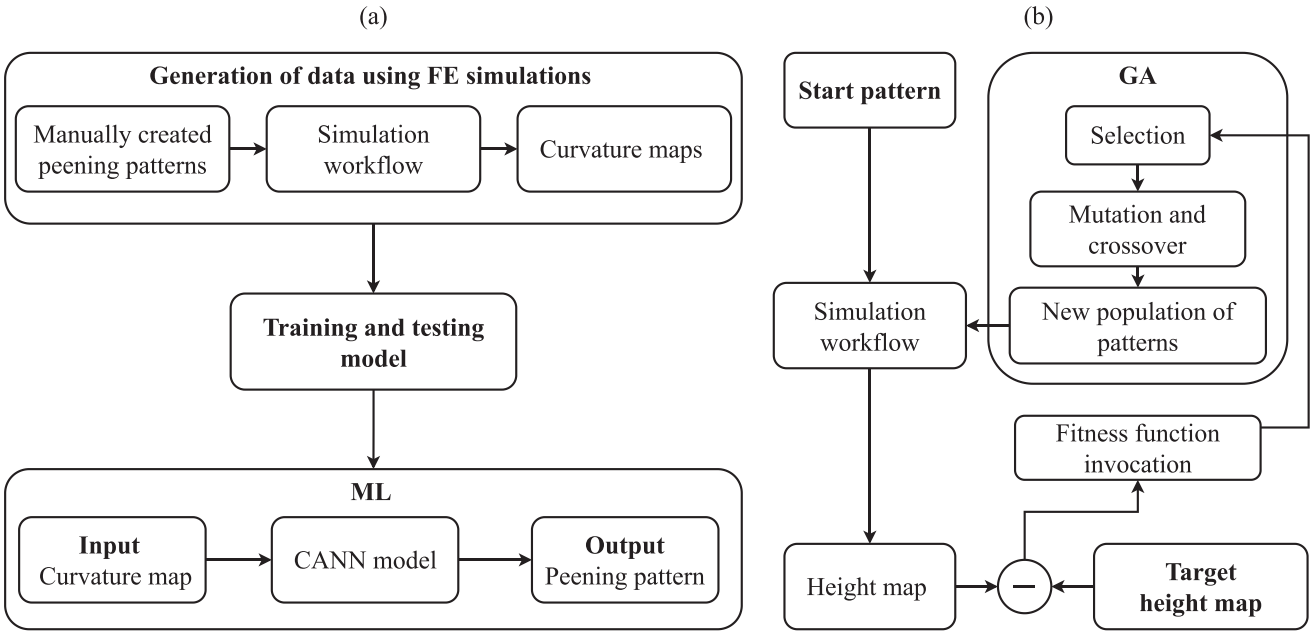

Fig. 2. Schematic of proposed ML and GA techniques to predict the peening pattern required to achieve the desired deformation by LPF. (a) Training/testing data is generated by manually creating patterns using the FE workflow. A trained CANN model predicts peening patterns for given curvature maps. (b) GA approach iteratively calculates the error between simulation and target height maps. Peening patterns evolve through mutation and crossover functions, converging towards the target pattern.

an ML approach using CANN [13] and a GA-based approach [5]. The ML approach is novel and addresses the inverse problem directly, while the GA approach, a proven method in the literature [3] for complex mechanical problems, iteratively solves the direct problem until an optimal solution is reached. Unlike CANN, GA enables solving non-unique problems with multiple similar-quality solutions. Efforts have been made to decrease the computational time of the GA method, resulting in predicted patterns that closely align with the actual patterns. The results and limitations corresponding to both approaches are discussed.

2. Material and methods

This study proposes the development of a simplified linear-elastic predictive FE model for simulating the bending of 1 mm thick Ti-6Al-4V specimens (80 × 20 mm^2) during LPF. The objective is to generate simulation data, that is sufficiently accurate in representing the deformations caused by the peening pattern, enabling an effortless integration into data-driven approaches. The FE model developed in this study employed a linear-elastic approach using Abaqus FE software. The mesh consisted of 53667 linear C3D8R elements, providing sufficiently accurate and consistent predictions. The material parameters for the model were obtained from the literature [12].

Being a linear-elastic predictive model, the objective is to determine appropriate stress values to be applied as the initial stress at elements on the specimen corresponding to the peened region. A relaxation step allows the specimen to relax resulting in a residual deformation. The applied stress governs the deformation in the specimen. The deformed shape obtained from FE simulation must match the actual deformation achieved through LPF treatment. Bayesian optimization, a black-box optimizer, is employed to determine the optimal value of stress to be applied in the peened region, by minimizing the mean squared error (MSE) of displacement between the height map of simulated and experimental specimens iteratively until a tolerance level is reached. A workflow is established (see Fig. 1) to utilize this simplified FE model for obtaining deformations for different peening patterns that are consistent with the measured deformations obtained from experiments. The chosen representation of deformation after LPF is the curvature for CANN [16] and the height map for GA. Curvature is selected due to its orientation independence and correlation with patterns, making it easier to train the CANN. Height maps are chosen for the GA approach as they provide the desired information without cumulative error. For evaluating the workflow, LPF experiments were performed with an Nd:YAG laser with a square cross-section of 1 mm^2 at focus, producing a Gaussian beam profile width of 20 ns (full width at half maximum (FWHM)), using a laser power density of 12 GW/cm^2, 4 repetitions, and without using a protective overlay (see Fig. 1). The peening pattern was created by moving the sample relative to the laser across the specimen's width, forming one peening line. This was repeated four times within a single peening line. Then, the specimen was repositioned along its length with an offset of 1 mm to start the next peening line. This process was iterated to generate the desired peening pattern. The optimizer predicted an initial stress value of −320 MPa on the surface for the stated experimental parameters.

The ML approach (Fig. 2(a)) utilizes a CANN architecture [13] to learn rules by which individual cells (or pixels representing single shots) can classify themselves into the correct peening pattern i.e. the state of either being peened or not peened when provided with the curvature of the specimen. To ensure generalization, this approach necessitates a diverse set of peening patterns for training and evaluation. A total of 31 diverse set of peening patterns that the model could encounter in real-world applications and their corresponding curvatures were utilized, with 22 patterns for training and the rest for evaluating the ML model. To avoid duplicate simulations, unsymmetrical patterns were mirrored. In addition to the curvature of the specimen, the curvature at the edges, when peened, was exclusively provided to ensure that the trained model can differentiate the edges from the rest of the specimen. After sufficient training on various peening patterns, this ML model effectively identifies the peening pattern when presented with a curvature map.

The GA approach in this study solves the inverse problem iteratively by treating it as a forward problem. A population of chro-

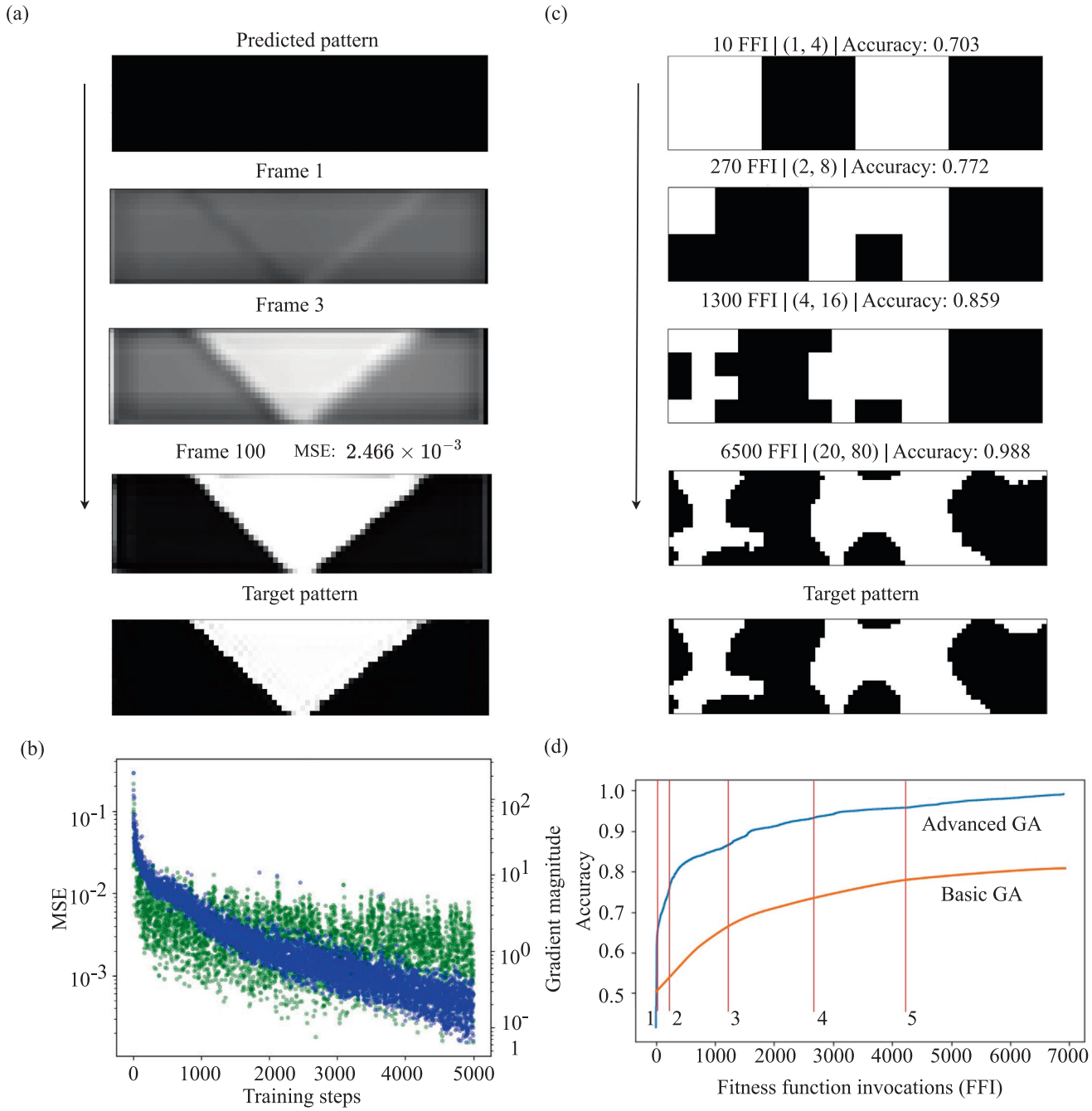

Fig. 3. Predicted peening patterns in ML and GA approaches: (a) The evolution of predicted peening pattern with the increasing number of iterations of the CANN model. (b) The loss (MSE) and gradient magnitude during the training of the CANN model. (c) The progression in predicted peen pattern through multiple sub-divisions in the pattern upon increasing FFI's in the advanced GA. (d) Comparison of accuracy of the basic GA and advanced GA. The vertical lines indicate the FFI at which the sub-division of the pattern changed.

mosomes is generated, with each chromosome consisting of 1600 genes (signifying dimensions of the specimen) representing the peened (state 1) or not peened (state 0) regions. The fitness of each chromosome is evaluated by a sequence of steps described in Fig. 2 (b), and by calculating the MSE of the generated height map. The hyper-parameters tuned by the GA include the number of solutions per generation, the number of parents selected for mating, the number of parents kept for the next generation, the mutation probability, and the number of generations, with considerations for minimizing fitness function invocations and preventing loss of good genes while limiting the maximum number of fitness function invocations when there is no improvement. Attempts were made to ensure faster convergence by utilizing subdivisions and advanced GA mutation features implemented in PyGAD [5].

3. Results and discussion

The ML methodology employed various peening patterns after experimental validation for the specified set of LPF process parameters. Fig. 3(a) illustrates the progression of the prediction for an exemplary peening pattern in the test dataset after training the CANN, demonstrating a good agreement between the predicted pattern and the target pattern (ground truth). The MSE depicted

in Fig. 3(a) indicates a decreasing loss from 10^{-1} to 5×10^{-4} as training advances. The evolution of the gradient reflects changes in the model's weights and biases during training, with a larger magnitude signifying significant alterations in these parameters. The results reveal that the CANN model has inherent limitations: being trained solely on curvatures from diverse peening patterns for a single LPF process parameter, it exhibits poor extrapolation capabilities common to neural networks [1] and lacks the ability to generate patterns for curvatures beyond the training distribution.

The generalization problem can be effectively addressed by employing the GA approach, which repeatedly solves the direct problem in order to achieve the optimal solution. As a result, the GA approach is applicable to various sets of LPF process parameters and curvatures. Nevertheless, it is important to note that satisfactory outcomes can only be obtained by allowing sufficient runtime for this approach. The fundamental GA approach identifies the appropriate peening pattern by making random determinations regarding the peening or non-peening of individual cells (there are 80×20 cells that represent the dimension specimens). As illustrated in Fig. 3(d), the patterns reach a point where further improvements become negligible after 40000 FFI, achieving an accuracy of 87%. Assessing the FFI of a particular pattern necessitates approximately 40 seconds, thereby demanding a computation time of approximately 2.7 weeks which is exceptionally high.

The computation time is substantially reduced by utilizing an advanced GA with sub-divisions. Sub-divisions involve dividing a coarse version of the pattern into high resolution, ranging from (4,1) to (80,20). This approach forces the GA to begin with simpler solutions, increasing the sub-divisions gradually until reaching the desired pattern. The accuracy of the GA improves notably with increasing sub-divisions, as shown in Fig. 3(c). The advanced GA approach shows an improvement in the accuracy from 70 % to 90 % after 2800 FFI which reduces the computation time from weeks to 1.3 days.

4. Conclusion and outlook

The present work aimed to find an algorithm for acquiring a peening pattern for LPF that induces a target deformation. A workflow comparing FE simulations and experimental results is developed. Two approaches, ML, and GA, were explored. The ML approach using CANN showed accuracy for specific deformations but struggled with patterns outside the training regime. The GA approach gave acceptable solutions but had limitations in computation time and the tendency to generate sparse and noisy patterns, which was solved by starting with coarser patterns and subsequent subdivisions. Additionally, the GA approach can be optimized further to reduce computation time, such as stopping the simulation at a lower resolution or applying post-processing algorithms to compensate for the noise.

Declaration of Competing Interest

The authors declare that they have no known competing financial interests or personal relationships that could have appeared to influence the work reported in this paper.

Acknowledgements

Author Contributions: **S. T. S., R. K., N. H.,** and **N. K.** conceptualized the study; methodology, investigation, and visualization were conducted by **R. K.**; resources were gathered by **N. H.** and **N. K.**; **S. T. S.** did the writing –original draft preparation; **S. T. S., R. K., N. H.,** and **N. K.** did the writing –review, and editing; **N. H., N. K.,** and **S. T. S.** supervised the study. All the authors have read and agreed to the published version of the manuscript.

Appendix A. Supplementary material

Supplementary data associated with this article can be found, in the online version, at https://doi.org/10.1016/j.mfglet.2023.09.006.

References

[1] Courtois A, Morel J-M, Arias P. Can neural networks extrapolate? discussion of a theorem by pedro domingos. Revista de la Real Academia de Ciencias Exactas, Físicas y Naturales. Serie A. Matemáticas 2023;117(2).
[2] Ding H, Shen N, Li K, Bo W, Pence CN, Ding H. Experimental and numerical analysis of laser peen forming mechanisms of sheet metal. In: Volume 2: Processing. American Society of Mechanical Engineers; 2014.
[3] Elaziz MA, Elsheikh AH, Oliva D, Abualigah L, Lu S, Ewees AA. Advanced metaheuristic techniques for mechanical design problems: Review. Arch Comput Methods Eng 2021;29(1):695–716.
[4] Faucheux PA, Gosselin FP, Lévesque M. Simulating shot peen forming with eigenstrains. J Mater Process Technol 2018;254:135–44.
[5] Gad AF. Pygad: An intuitive genetic algorithm python library; arXiv;2021.
[6] Hu Y, Grandhi RV. Efficient numerical prediction of residual stress and deformation for large-scale laser shock processing using the eigenstrain methodology. Surf Coat Technol 2012;206(15):3374–85.
[7] Hu Y, Han Y, Yao Z, Hu J. Three-dimensional numerical simulation and experimental study of sheet metal bending by laser peen forming. J Manuf Sci Eng 2010;132(6).
[8] Hu Y, Jiang J, Tang X. Peening pattern optimization with integer eigen-moment density for laser peen forming of complex shape. Struct Multidiscip Optim 2023;66(4).
[9] Hu Y, Luo M, Hu L, Yao Z. Efficient process planning of laser peen forming for complex shaping with distributed eigen-moment. J Mater Process Technol 2020;279:116588.
[10] Hu Y, Xu X, Yao Z, Hu J. Laser peen forming induced two way bending of thin sheet metals and its mechanisms. J Appl Phys 2010;108(7):073117.
[11] Hu Y, Zheng X, Wang D, Zhang Z, Xie Y, Yao Z. Application of laser peen forming to bend fibre metal laminates by high dynamic loading. J Mater Process Technol 2015;226:32–9.
[12] Lee W-S, Lin C-F. High-temperature deformation behaviour of Ti6Al4V alloy evaluated by high strain-rate compression tests. J Mater Process Technol 1998;75(1–3):127–36.
[13] Mordvintsev A, Randazzo E, Niklasson E, Levin M. Growing neural cellular automata. Distill 2020;5(2).
[14] Pöltl D, Keller S, Chupakhin S, Sala ST, Kashaev N, Klusemann B. Numerical investigation of influence of spot geometry in laser peen forming of thin-walled Ti-6Al-4V specimens. Key Eng Mater 2022;926:2293–302.
[15] Sala ST, Keller S, Chupakhin S, Pöltl D, Klusemann B, Kashaev N. Effect of laser peen forming process parameters on bending and surface quality of Ti-6Al-4V sheets. J Mater Process Technol 2022;305:117578.
[16] Siguerdidjane W, Khameneifar F, Gosselin FP. Efficient planning of peen-forming patterns via artificial neural networks. Manuf Lett 2020;25:70–4.